

## Electronic structure of PbSe and PbTe. I. Band structures, densities of states, and effective masses\*

G. Martinez, M. Schlüter,<sup>†</sup> and Marvin L. Cohen

Department of Physics, University of California and Inorganic Materials Research Division, Lawrence Berkeley Laboratory, Berkeley, California 94720

(Received 14 October 1974)

We present new improved pseudopotential calculations for PbSe and PbTe using several nonlocal corrections in addition to the local empirical pseudopotential. We discuss results for effective masses, Knight-shift measurements, and recent photoemission measurements. In addition to the optical properties in an energy range from 0 to 20 eV (which will be discussed in a subsequent paper), all the above experimental results can for the first time be explained consistently using *one* band-structure model.

### I. INTRODUCTION

A large number of band structures of the lead chalcogenides have already been calculated, using various methods. The orthogonalized-plane-wave (OPW) method has been employed by Herman *et al.*,<sup>1</sup> the augmented-plane-wave (APW) method by several authors<sup>2-4</sup> and the Korringa-Kohn-Rostoker (KKR) method by Overhof and Rössler.<sup>5</sup> Two different versions of the pseudopotential method have also been published; one of them including a strong nonlocal *s*-like potential<sup>6,7</sup>—of the Lin-Kleinman form and one being purely local—the empirical pseudopotential method (EPM).<sup>8</sup> None of these calculations was able to give an overall coherent picture of the physical properties of PbSe and PbTe. In particular, only Bernick and Kleinman<sup>7</sup> were able to reproduce the effective masses, whereas only the EPM<sup>8</sup> results yielded optical results in agreement with experiment. Furthermore, the appearance of recent XPS and UPS measurements<sup>9,10</sup> revealed general disagreements with all published band structures. We have thus reopened this problem in an attempt to obtain acceptable agreement with all known experimental measurements.

To perform the calculations we have chosen the EPM which uses a local empirical pseudopotential. This local potential had to be modified by adding an effective mass to the kinetic energy operator and by adding a full nonlocal *d* potential. A detailed description of this procedure is given in Sec. II. The resulting band structures are presented in Sec. III, together with a justification of the form of the potential used and a discussion of the parameters involved. In Sec. IV we compare the physical properties near the fundamental absorption edge to experimental results. Section V is devoted to the calculation of the density of states of the valence bands and to a comparison of these results with experimental photoemission data. The study of the optical properties in an energy range from 0 to 20 eV will be presented in a subsequent paper.<sup>11</sup>

### II. BAND-STRUCTURE CALCULATIONS

The band-structure calculations were done using the empirical pseudopotential method (EPM). This approach is well established and discussed extensively in the literature.<sup>12</sup> Briefly, the method involves the solution of a pseudopotential Hamiltonian

$$H = -\Delta + V_L(\vec{r}) + V_{NL}(\vec{r}), \quad (1)$$

whose local pseudopotential  $V_L(\vec{r})$  is expanded in the reciprocal lattice

$$V_L(\vec{r}) = \sum_{\vec{G}} V(\vec{G}) e^{i\vec{G}\cdot\vec{r}}, \quad (2)$$

where  $\vec{G}$  is a reciprocal-lattice vector. For the case of crystals with rock-salt structure  $V(\vec{G})$  can be divided into symmetric and antisymmetric contributions

$$V(\vec{G}) = V_S(|\vec{G}|) S_S(\vec{G}) + V_A(|\vec{G}|) S_A(\vec{G}), \quad (3)$$

where  $V_S$  and  $V_A$ , the symmetric and antisymmetric form factors, are treated as empirical parameters. They are related to the atomic form factors  $V_c$  and  $V_a$  of cation and anion by

$$V_S = \frac{1}{2}(V_c + V_a) \quad \text{and} \quad V_A = \frac{1}{2}(V_c - V_a). \quad (4)$$

$S_S$  and  $S_A$  denote the corresponding symmetric and antisymmetric structure factors. The nonlocal potential  $V_{NL}(\vec{r})$  in Eq. (1) contains two different contributions, (a) a nonlocal and (generally energy-dependent) correction  $W$  to the local atomic pseudopotential  $V_L$  as derived, e.g., from the usual OPW formalism,<sup>13</sup> and (b) a relativistic correction  $R$  which describes the spin-orbit interaction. Only the spin-orbit-interaction part of the relativistic correction is added explicitly, for this interaction breaks the symmetry of the nonrelativistic Hamiltonian. Other relativistic terms have full symmetry and can be considered to be absorbed into the nonrelativistic empirical pseudopotential.

In the usual plane-wave representation, the nonlocal energy-dependent pseudopotential becomes formally  $W(\vec{k} + \vec{G}, \vec{k} + \vec{G}', E)$ . It is believed that the

first-order influence on the band structure of  $W$  can be accounted for by retaining only main-diagonal terms, i.e., terms with  $\vec{G} = \vec{G}'$ . Moreover, it has been shown<sup>12</sup> that in this case nonlocality and energy dependence can be simulated by the introduction of an effective mass  $m^* = m_K m_E$ . In terms of  $W(\vec{k}, \vec{K}, E)$ ,  $m_K$  and  $m_E$  can be expressed as

$$m_K^{-1} = 1 + \frac{1}{|\vec{k}|} \frac{\partial W}{\partial k}, \quad m_E = 1 - \frac{\partial W}{\partial E}, \quad (5)$$

where the derivatives are usually taken at the Fermi level. In an actual band-structure calculation  $m^*$  can either be treated as an empirical parameter or it can be calculated from nonlocal atomic model potentials.<sup>14</sup> In the latter case the value of  $m^*$  entering the crystal Hamiltonian has to be computed according to the linear additive behavior of  $W$  for different atoms. Even though this effective-mass treatment appears to be a very crude approximation to the "true" nonlocality, it nevertheless simulates  $s$ - $p$  nonlocality to some extent. Since  $1/m^*$  scales the kinetic energy, it influences the energy separation of the low-lying ( $s$ -like) states differently from the higher-lying (mostly  $p$ - and  $d$ -like) states. It follows from the different localization of nonlocal potentials in  $K$ -space (we shall discuss this point in Sec. III) that retaining only main-diagonal terms of  $W$  is a better approximation for  $s$ - $p$  nonlocality than it is for  $d$  nonlocality. It seems therefore desirable to include  $d$  nonlocality in a more explicit way, e.g., by retaining off-diagonal terms of  $W$  as well.

A typical form for the  $d$ -like nonlocal potential can be obtained from the original OPW Hamiltonian.

$$\langle \vec{k} + \vec{G} | W_i^d | \vec{k} + \vec{G}' \rangle = A_i \langle \vec{k} | t_i \rangle \langle t_i | \vec{k}' \rangle, \quad (6)$$

where  $\vec{K} = \vec{k} + \vec{G}$ , and where  $|t_i\rangle$  should include all  $d$ -like core states of atoms of type  $i$ . In practice, however, only  $d$ -like states of the *last* filled core shell have to be considered, since the overlap matrix elements in (6) decrease by about one order of magnitude with each core shell. The simulation of  $d$ -like nonlocal potentials using Eq. (6) introduces one additional parameter for each kind of atom. The integrals in Eq. (6) can be evaluated by taking atomic-core wave functions<sup>15</sup>  $R_{n_l}(r)$ ; Eq. (6) then becomes

$$\begin{aligned} \langle \vec{k} + \vec{G} | W_i^d | \vec{k} + \vec{G}' \rangle \\ = A_i \frac{4\pi(2l+1)}{\Omega_0} P_l(\cos\alpha) B_{n_l}^i(|\vec{k}|) B_{n_l}^i(|\vec{k}'|) \\ \times S_i(\vec{G}' - \vec{G}), \quad l=2, \end{aligned} \quad (7)$$

where  $\Omega_0$  denotes the unit cell volume,  $P_l$  a Legendre polynomial, and  $\alpha$  the angle between  $\vec{k} + \vec{G}$  and  $\vec{k} + \vec{G}'$ .  $S_i(\vec{G}' - \vec{G})$  represents the usual structure factor for atoms of type  $i$ , and

$$B_{n_l}^i(|\vec{k}|) = \int_0^\infty R_{n_l}^i j_l(|\vec{k}|r) r^2 dr$$

is a slowly varying function of  $|\vec{k}|$ , depending on atomic radial functions  $R_{n_l}^i$  and on spherical Bessel functions  $j_l$ .

The nonlocal relativistic correction  $R$  can be derived from a spin-orbit Hamiltonian of the form

$$H_{so} = (\hbar/4m^2c^2)[\vec{\nabla} V(\vec{r}) \times \vec{p}] \cdot \vec{\sigma}, \quad (8)$$

where  $V(\vec{r})$  is the real crystal potential,  $\vec{p}$  is the momentum operator, and  $\vec{\sigma}$  is the Pauli spin operator. Following a procedure described by Weisz,<sup>16</sup> we can derive the matrix element appearing in the pseudopotential Hamiltonian,

$$R(\vec{k}', s'; \vec{k}, s) = \sum_i \vec{\sigma}_{s',s} (\vec{\Lambda}_p^i + \vec{\Lambda}_d^i) S_i(\vec{k} - \vec{k}'), \quad (9)$$

where  $S_i$  are atomic structure factors and  $\vec{\sigma}_{s',s} = \langle s' | \vec{\sigma} | s \rangle$  are matrix elements in spin space. The nonlocal potentials

$$\vec{\Lambda}_p^i = 12\pi \frac{-i\lambda_p^i}{\Omega_0} B_{n,1}^i(|\vec{k}|) B_{n,1}^i(|\vec{k}'|) \frac{\vec{k}' \times \vec{k}}{|\vec{k}'| |\vec{k}|}, \quad (10)$$

$$\vec{\Lambda}_d^i = 60\pi \frac{-i\lambda_d^i}{\Omega_0} B_{n,2}^i(|\vec{k}|) B_{n,2}^i(|\vec{k}'|) \frac{(\vec{k}' \times \vec{k})(\vec{k}' \cdot \vec{k})}{|\vec{k}'|^2 |\vec{k}|^2},$$

represent the core spin-orbit interactions projected on the valence pseudo-wave-function. Nonlocality enters Eq. (10) via the vector product  $(\vec{k}' \times \vec{k})$  for the  $p$ -like contribution and via  $(\vec{k}' \times \vec{k}) \cdot (\vec{k}' \cdot \vec{k})$  for the  $d$ -like contribution. This reflects the different angular behavior of  $p$  and  $d$  functions. The functions  $B_{n,i}^i(|\vec{k}|)$  are the radial integrals which appeared in Eq. (7).

As mentioned in the discussion of Eq. (6), only the outermost core shell has to be considered in the calculation of the overlap integrals. The empirical parameters  $\lambda_p^i$ ,  $\lambda_d^i$  determine the strength of the spin-orbit coupling in the crystal. With the assumption that the ratio of these parameters for different atoms  $i$  in the crystal is the same as for the free atoms, we end up with two parameters  $\lambda_p$  and  $\lambda_d$  describing the spin-orbit interaction in the crystal.

### III. RESULTS FOR THE BAND STRUCTURES AND DISCUSSION OF IMPORTANT PARAMETERS

The parameters used in our band-structure calculations are presented in Table I. The resulting  $E(\vec{k})$  curves are shown in Fig. 1 for PbSe and in Fig. 2 for PbTe.

The lattice parameter  $a$  has been taken from x-ray measurements at 4 °K for PbTe<sup>17</sup> and has been computed from the experimental dilation coefficient as a function of temperature,<sup>18</sup> together with the room-temperature value of the lattice constant for



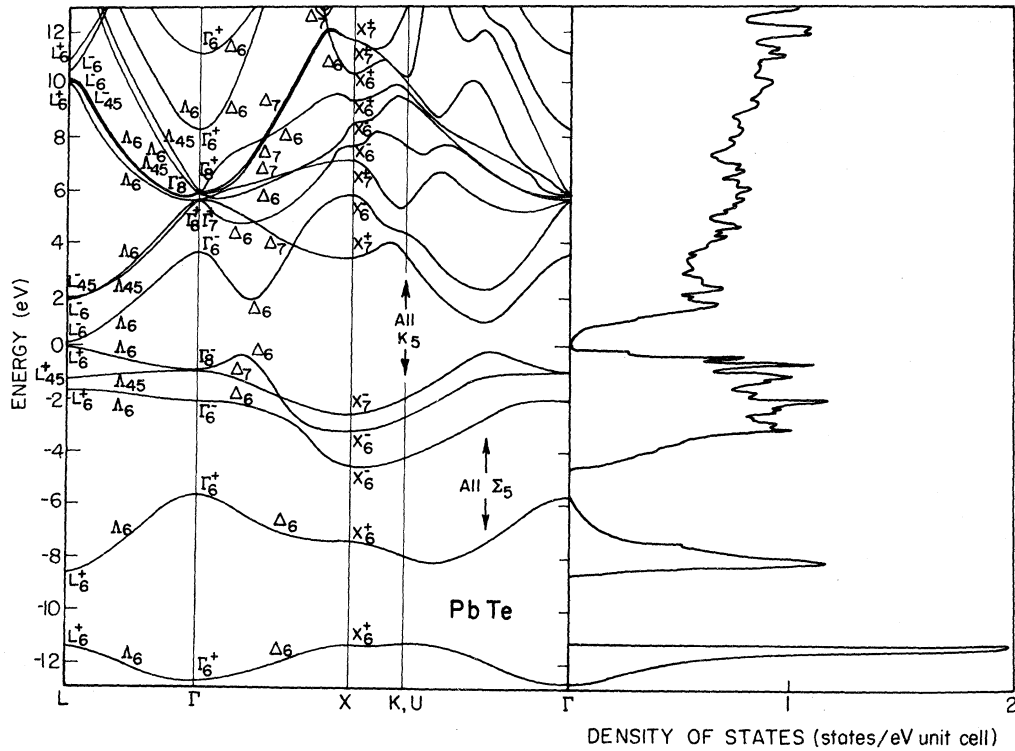


FIG. 2. EPM band structure of PbTe, together with the calculated density of states. The same symmetry notation is used as for Fig. 1.

with respect to different form factors:

$$\frac{\partial \Delta E}{\partial V_{24}} \sim -35, \quad \frac{\partial \Delta E}{\partial V_4} \sim -10, \quad \frac{\partial \Delta E}{\partial V_8} \sim -1.6.$$

In view of these results, we can believe that cutting off the local pseudopotential at some  $|\bar{G}|^2 < 24$  affects the band structure like a nonlocal *d-like* potential. It depends solely on the remaining local form factors whether this spurious nonlocal potential is attractive or repulsive.

For our calculation we choose a cutoff at  $G^2 = 16$ , which leads to an energy convergence of better than 0.025 eV. The lead potentials used in both salts are very similar, which is consistent with the fact that we do not expect a large difference in the screening between PbSe and PbTe. Comparing our cation and anion potentials, their difference in electronegativity is generally smaller than that reported in earlier publications.<sup>8</sup> This results in a decrease of the gap between the two low-lying valence *s* bands, which is, as we shall see in Sec. VI, in accordance with recent EPS and UPS data.

The effective-mass parameters have been chosen empirically. However, since these values should not depend on the particular screening, we expect them to be close to the values calculated from atomic model potentials. Appapillai and Heine<sup>14</sup>

have recently calculated optimized model potentials and effective masses for a number of atoms, including Pb, Se, and Te. They find the following masses: for Pb,  $m_k = 0.917$ ,  $m_E = 0.963$ ; for Se,  $m_k = 1.0002$ ,  $m_E = 0.975$ ; and for Te,  $m_k = 1.02$ ,  $m_E = 0.969$ . The corresponding effective masses for the compounds can be computed according to Eq. (5). Thus in the case of PbTe, for example, we find

$$m_k^{-1}(\text{PbTe}) = 1 + m_r^{-1}(\text{Pb}) - 1 + m_r^{-1}(\text{Te}) - 1,$$

$$m_E(\text{PbTe}) = 1 + m_E(\text{Pb}) - 1 + m_E(\text{Te}) - 1.$$

From that we obtain the values

$$m_k(\text{PbTe}) = 0.934, \quad m_E(\text{PbTe}) = 0.932,$$

$$m^*(\text{PbTe}) = 0.870,$$

$$m_k(\text{PbSe}) = 0.917, \quad m_E(\text{PbSe}) = 0.944,$$

$$m^*(\text{PbSe}) = 0.866.$$

Considering the uncertainty involved in this kind of calculation, which is essentially given by the inaccurate determination of the energy slope of the model-potential parameters, we can say that these values are in good agreement with our empirical findings (see Table I).

We shall now discuss in more detail the influence of the use of effective masses on the band-structure results. The concept of introducing effective masses is to reproduce nonlocality at  $\vec{G}=0$ , which is equivalent to considering only main-diagonal matrix elements of the nonlocal potential. The validity of this approach, however, demands that the off-diagonal terms have to be small compared to the diagonal terms. In other words, one has to assume that in Eq. (6),  $|\langle \vec{K} | t \rangle|^2$  is larger than  $\langle \vec{K} | t \rangle \langle t | \vec{K} + \vec{G}' \rangle$  for most of the  $\vec{G}'$  vectors (we have set  $\vec{k} + \vec{G} = \vec{K}$ ). This turns out to be a reasonable assumption for  $s$  and  $p$  states, but it becomes questionable for  $d$  states. This results from the extension in  $\vec{K}$  space of the matrix element  $\langle \vec{K} | t \rangle$ . For a mean value of  $|\vec{K}|$  (such as  $\vec{K}^2 = 8$ ),  $\langle \vec{K} | t \rangle$  is still an increasing function of  $|\vec{K}|$  for  $d$  states, and in some cases the off-diagonal terms are even bigger than the diagonal terms. The effective-mass approach therefore does not seem to be a sufficiently accurate treatment for  $d$  nonlocality.<sup>19</sup>

This fact, together with the remarks concerning the cutoff of the local pseudopotential, justifies the inclusion of a complete nonlocal  $d$ -like potential into the calculation of the band structures. However, the repulsive or attractive character of this potential can only have a relative meaning with respect to the local empirical potentials which we used. For this reason we shall not try to attribute any physical meaning to the fact that we used an attractive potential for lead (for PbTe) and a repulsive one for selenium (for PbSe). In Table I we give the values  $A_i$  according to Eq. (7) for the nonlocal pseudopotentials used in our calculations. These values might at first sight appear to be very large. However, to compare them with the local form factors, they have to be corrected by several factors arising from the functions  $B_{n_i}^i$  in Eq. (7) and from the volume  $\Omega_0$ . The comparable values are thus  $-0.0044$  Ry for PbTe and  $+0.0019$  Ry for PbSe. Compared to the local pseudopotential, these values are quite small, as they should be if they are to remain a small correction to the basic local scheme. The influence on the band structure of these corrections is essential only to reproduce the optical properties of these two compounds above 6 eV. This will be discussed in detail in a subsequent paper.<sup>11</sup> We should add on this particular point that all the arguments given here to support the introduction of a nonlocal  $d$ -like potential are quite general and should be valid for most semiconductors. Although for some cases the introduction of an effective mass is not justified, e.g., Si, where theoretically  $m^* = 0.999$ ,<sup>14</sup> there still remains the cutoff of the local pseudopotential, which should by itself justify the use of a nonlocal  $d$ -like potential.

Though Si calculations<sup>13</sup> performed without a

nonlocal  $d$ -like potential have succeeded in reproducing the optical properties for energies up to 6 eV, the  $d$ -like potential might be necessary to reproduce the optical properties at higher energies. Furthermore, our arguments do not exclude a case in which the cutoff of the higher- $|\vec{G}|$  form factors can accidentally be absorbed by the remaining form factors.

The spin-orbit parameters have also been chosen empirically in such a way that the splitting  $\Gamma_6^- - \Gamma_8^-$  of the upper valence bands correspond to that found by the OPW method.<sup>1</sup> As inferred from atomic values, the  $d$  contribution to the spin-orbit splitting is quite negligible and can be left out to simplify the calculations.

#### IV. EFFECTIVE MASSES

The lead salts exhibit a small direct gap at the point  $L$  of the Brillouin zone. It is known that the properties connected with this gap can only be explained by taking into account the mass anisotropy and the strong nonparabolicity of the bands around the gap energy. In the following we shall discuss only the effect of anisotropy. For this discussion it is essential to know the values of the effective masses at  $L$ . The experimental values are given in Table II for PbSe and PbTe.<sup>20</sup> The most striking feature seems to be the large difference in the anisotropy of the masses for longitudinal (parallel to  $\Gamma L$ ) and transverse (perpendicular to the  $\Gamma L$ ) direction between the two salts. It is known<sup>21,22</sup> that a  $\vec{k} \cdot \vec{p}$  theory around  $L$  including only six bands can reproduce quite well the band structure and the associated physics in this energy range. On the basis of this theory we expect, owing to the large difference in the mass anisotropy between PbSe and PbTe, a noticeable change in the bands around the  $L$  point. Bernick and Kleinman<sup>7</sup> were the first to propose an inversion of the two  $L_6^-$  levels forming the first two conduction bands going from PbSe to PbTe. The reason for this can be understood in the  $\vec{k} \cdot \vec{p}$  framework if we write down the expression for the effective masses and look at the origin of the six bands in a scheme without spin-orbit interaction (Fig. 3). Without

TABLE II. Calculated and experimental (Ref. 20) effective masses for PbSe and PbTe given in units of free-electron masses.

	PbSe		PbTe	
	Experiment	Calculation	Experiment	Calculation
$m_1^v$	$0.068 \pm 0.015$	0.083	$0.31 \pm 0.05$	0.265
$m_2^v$	$0.034 \pm 0.007$	0.030	$0.022 \pm 0.003$	0.0232
$m_3^v$	$0.070 \pm 0.015$	0.077	$0.24 \pm 0.05$	0.219
$m_4^v$	$0.040 \pm 0.008$	0.032	$0.024 \pm 0.003$	0.0225

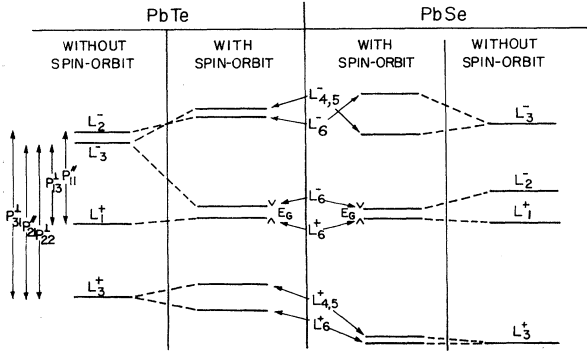


FIG. 3. Band configurations with and without spin-orbit interaction around the fundamental absorption edge for PbSe and PbTe. The nonzero matrix elements of the crystal momentum in the absence of spin-orbit coupling are shown schematically for the longitudinal ( $\parallel$ , i. e., parallel to  $\Gamma L$ ) and the transverse ( $\perp$ , i. e., perpendicular to  $\Gamma L$ ) directions. The notation is that of Mitchell and Wallis (Ref. 24).

spin-orbit interaction there remain only four bands and the  $p$ -matrix elements which couple these bands have well defined polarization ( $\perp$  and  $\parallel$ ) as shown in Fig. 3. It turns out from actual calculations that  $P_{13}^{\perp}$  or  $P_{31}^{\perp}$  are larger than  $P_{11}^{\parallel}$  by about a factor of 3. Thus, if the lowest  $L_6^-$  level originates from  $L_2^-$ , we expect, owing to the difference between the relative energies, a compensation for the difference in the values of the matrix elements for the two polarizations, and consequently a relatively weak mass anisotropy. This should clearly be the PbSe case. On the other hand, if the lowest  $L_6^-$  level originates from an  $L_3^-$  level, we expect an accumulative effect and longitudinal masses much larger than the transverse ones. This is the case for PbTe.

We found in this framework that this band ordering represents the only solution which can explain the very different experimentally observed anisotropies. In particular, we shall show in a later publication<sup>23</sup> that with this particular ordering the pressure dependence of the gap can be well understood. The calculated effective masses at  $L$  are given for comparison in Table II. They have been calculated by fitting a parabola very closely to the  $L$  point (in the longitudinal and in the transverse direction) in the band structure. This procedure appears to be necessary to obtain accurate masses because the values of the matrix elements are known only within an error of about 10%. Owing to the particular structure of the expression for the effective masses in the  $\vec{k} \cdot \vec{p}$  theory, any error in the matrix elements connecting the two levels at the gap is considerably enhanced by the small

value of this gap, thus strongly affecting the values of the effective masses.

## V. KNIGHT-SHIFT EXPERIMENTS

Knight-shift measurements on  $\text{Pb}^{207}$  in PbSe and PbTe have been reported<sup>25</sup> recently. Their interpretation provides a very useful quantity, namely, the relative charge density at the lead site  $|\psi(0)|^2$  for the upper valence band at  $L$  (the experiments were done with  $p$ -type material). Owing to the relatively large uncertainties involved in the determination of the  $g$  factors, the values deduced for  $|\psi(0)|^2$  are known only within  $\pm 10\%$ . Within this uncertainty, the ratio of  $|\psi(0)|^2$  at the lead atom, normalized to the volume of the primitive cell, is found to be equal for both salts and about 0.67.

$|\psi(0)|^2$  corresponds essentially to the fractional  $s$ -like part of the wave function around the lead atoms at the top of the valence band. To evaluate this quantity we have expanded the plane-wave solutions of our EPM calculations in spherical harmonics. Then

$$\psi(\vec{r}) = \sum_{l=0}^L \psi_l(\vec{r}). \quad (11)$$

The sum in Eq. (11) was restricted to  $L=2$ , and all functions are normalized, neglecting higher angular moments. Then the  $l$  character,  $c^l = \langle \psi_l | \psi_l \rangle$ , of the wave function can be characterized by

$$c^l = 4\pi \sum_{\vec{G}, \vec{G}'} a_{\vec{G}}^* a_{\vec{G}'} (2l+1) P_l(\cos \alpha) \times \int_0^{R_l} j_l(|\vec{G} + \vec{k}|r) j_l(|\vec{G}' + \vec{k}|r) r^2 dr, \quad (12)$$

where  $P_l$  is the Legendre polynomial,  $\alpha$  is the angle between  $\vec{K} = \vec{G} + \vec{k}$ , and  $\vec{K}' = \vec{G}' + \vec{k}$ , and  $j_l(x)$  the spherical Bessel function of order  $l$ . The coefficients  $a_{\vec{G}}$  are the eigensolutions of the EPM calculation.  $R_l$  is the radius of a sphere around the atom under consideration in which we evaluate the charge density. The integration in (12) can be carried out analytically for all  $l$ . Here we are interested in the  $l=0$  case ( $s$  character) only. In this case we obtain

$$c^0 = 4\pi \sum_{\vec{G}, \vec{G}'} a_{\vec{G}}^* a_{\vec{G}'} \frac{1}{|\vec{K}|^2 |\vec{K}'|^2} \left( \frac{\sin(|\vec{K}|R) \cos(|\vec{K}'|R)}{|\vec{K}|} - \frac{\sin(|\vec{K}'|R) \cos(|\vec{K}|R)}{|\vec{K}'|} \right) \quad \text{for } |\vec{K}| \neq |\vec{K}'| \quad (13)$$

$$= 4\pi \sum_{\vec{G}, \vec{G}'} a_{\vec{G}}^* a_{\vec{G}'} \frac{1}{2|\vec{K}|^3} \times [|\vec{K}|R - \sin(|\vec{K}|R) \cos(|\vec{K}|R)] \quad \text{for } |\vec{K}| = |\vec{K}'|.$$

Clearly, this quantity depends on the value chosen for  $R$ . It turns out that  $c^0$  normalized to  $R_0^3$  passes through a minimum as a function of  $R$  at  $R = 1.20$  Å for PbSe and  $R = 1.25$  Å for PbTe. These values correspond well to the charge contours deduced from charge-density plots of the two salts, which will be discussed in a later publication.<sup>26</sup>

With these values of  $R$  the properly normalized values of  $c^0$  are found to be  $c^0(\text{PbTe}) = 0.61$  and  $c^0(\text{PbSe}) = 0.73$  around the lead atom for the top-most valence band at  $L$ . Owing to the aforementioned uncertainties in the experimental results, and to the fact that the calculations were done on the basis of *pseudo*-wave-functions, the agreement between theory and experiment is very good.

Another interesting piece of information provided by Knight-shift experiments concerns *n*-type lead salts. The interpretation of these experiments reveals that the wave function of the first conduction band at  $L$  must have  $p^{1/2}$  character around lead for *both* compounds.

This is not in contradiction with the fact that the conduction bands have different origins for the two salts. This result is confirmed by our calculations. The information concerning the character of the lowest conduction bands will be very useful in determining the threshold energy for reflectivity measurements in the far uv involving transitions from the lead *d*-core levels into the conduction bands. Details of these experiments will be presented in a subsequent paper.<sup>11</sup>

## VI. X-RAY (XPS) AND ULTRAVIOLET (UPS) PHOTOEMISSION EXPERIMENTS

XPS and UPS experiments are believed to afford direct information about the density of states of

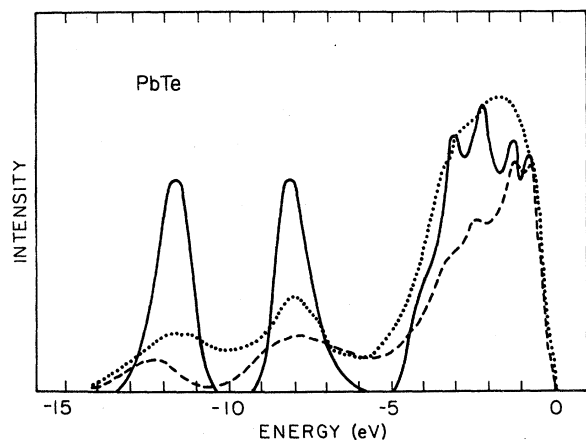


FIG. 4. XPS (Ref. 9) (dotted line) and UPS (Ref. 10) (dashed line) photoemission spectra of the valence-band structure of PbTe. Calculated densities of states are superimposed. The calculated curves are convoluted by an energy-dependent broadening function (see text).

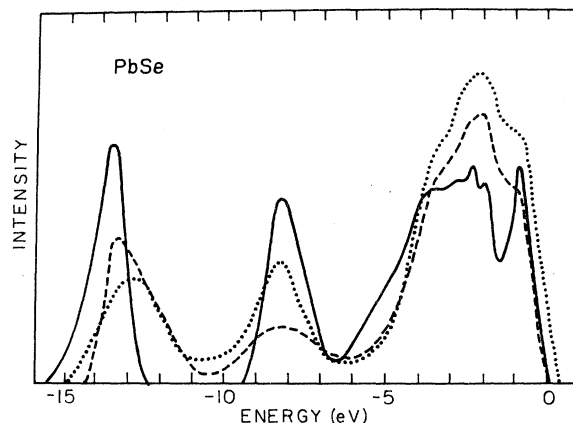


FIG. 5. XPS and UPS for PbSe; see caption of Fig. 4.

the valence bands. To calculate the densities of states from our EPM band structures we have used the method of Gillat and Dolling.<sup>27</sup>  $\vec{k}$ -space integration was done on the basis of 207 calculated points in the irreducible part ( $\frac{1}{48}$ ) of the Brillouin zone. Transition-matrix elements and energy gradients were calculated using  $\vec{k} \cdot \vec{p}$  techniques.

The resulting densities of states are presented in Figs. 1 and 2. First, we note that the density of states for the conduction bands is very uniform in both salts, and thus seems to indicate the free-electron-like behavior of these bands. This implication, however, proves to be incorrect, as is shown<sup>11</sup> when analyzing the spectra of core-to-conduction-band transitions, where it is found that the conduction-band states retain a significant amount of atomic character. As a further over-all feature we find the valence bands to be considerably broader in PbSe than in PbTe. We shall now compare our calculations with recently reported XPS<sup>9</sup> and UPS<sup>10</sup> measurements (Figs. 4 and 5). In these figures we have broadened the different groups of valence bands in the calculated curves with different broadening functions in order to facilitate the comparison with experiment. The three upper valence bands (*p* bands) have been broadened with a characteristic energy of 0.25 eV, the lead *s* band with an energy of 0.7 eV, and the lowest valence band (anion *s* band) with an energy of 1 eV. In addition, we give in Table III a quantitative comparison between our results and the experimental data by assigning the various structures to critical points in  $\vec{k}$  space. One of the difficulties encountered in the XPS or UPS measurements is to determine reference energies (i. e., the top of the valence bands). The reference energy is in general known only within  $\pm 0.4$  eV for XPS measurements and  $\pm 0.1$  eV for UPS measurements. In Figs. 4 and 5 we have therefore tried to align the

TABLE III. Comparison of structure in the XPS (Ref. 9) and UPS (Ref. 10) data with the calculated density of valence states and assignment to specific points in  $\bar{k}$  space. The  $\bar{k}$  point  $P'$  has the coordinates (0.71, 0.46, 0). All energies are given in eV and counted from the top of the valence bands. The XPS data on PbSe have been shifted by 0.3 eV towards lower energies to compensate for an error in the location of the Fermi level (see text). The theoretical energies in parenthesis are those obtained after the broadening (see text).

	Structures in XPS (Ref. 9) measurements	Structures in UPS (Ref. 10) measurements	Structures in EPM calculations	Assignment
PbTe		-0.65	-0.4(-0.6)	$\Delta(5), A(5)$
		-1.1	-0.9(-1.1)	$\Gamma(4, 5)$
	-2.3	-2.4	-1.8 } (-2.0)	$\Lambda(3)$
			-2.2 } (-2.0)	$\Delta(3), X(5)$
			-3.05(-2.9)	$X(4)$
	-8.20	-8.3	-8.25(-8.0)	$\Sigma(2), L(2)$
	-11.7	-12.5	-11.3(-11.6)	$X(1), K(1)$
PbSe	-0.9	-0.8	-1.0(-0.85)	$P'(5)$
	-1.90	-2.2	-2.0(-1.90)	$\Gamma(4, 5), \Lambda(4)$
			-2.4(-2.30)	$\Gamma(3)$
			-2.8(-2.80)	$\Delta(3)$
		-3.35	-3.3(-3.4)	$\Delta(4), \Sigma(3)$
			-3.8(-4.0)	$X(5)$
	-8.3	-8.3	-8.4(-8.3)	$P'(2), \Sigma(2)$
	-12.6	-13.4	-13.2(-13.5)	$X(1), K(1)$

peak energies of the  $s$ -lead bands (second valence band) which tends to give better agreement between the peak energies of the  $p$  bands of the two experimental curves than the quoted energy zeros. This, however, also shows that the given reference energy for the XPS measurements of PbSe is probably too large by 0.3 eV. On the other hand, the two lower peaks in the experimental curves are obtained after subtraction of a large background and therefore could be affected by a possible error ex-

ceeding the tolerance of  $\pm 0.1$  eV given in Ref. 9. Furthermore, all results are obtained with an experimental resolution of about 0.5 eV, which has to be taken into account in comparing our calculations to experiment. In view of these possible errors, the agreement between theory and both experiments is excellent.

## VII. CONCLUSION

We have presented calculations on the electronic structure of the lead chalcogenides PbSe and PbTe, which for the first time are in excellent agreement with existing experimental results. The different anisotropies of the effective masses at the band gap at the point  $L$  can be reproduced very accurately and can be explained by different band-ordering effects. Knight-shift data giving information about the character of the wave functions at both valence- and conduction-band edges can be well understood by analyzing the pseudo-plane-waves in terms of angular momentum eigenfunctions. Finally, the calculated density of states for valence bands is compared with recent XPS and UPS measurements. The agreement is excellent and deviations fall within the experimentally given tolerance. The reproduction of all these experiments, as well as of optical measurements in an energy range from 0 to 20 eV, which will be discussed in a subsequent paper, was achieved using empirical local pseudopotentials combined with an effective-mass parameter, simulating  $s$ - $p$  nonlocality and with a full nonlocal  $d$ -like potential. The latter potential only had to be included to obtain correct reflectivity data for energies above 6 eV.

\*Supported in part by the National Science Foundation Grant GH-35688.

†On leave from University of Paris VI, France, on NATO Fellowship. Permanent address: Laboratoire de physique des solides, Université Paris VI, 4 place Jussieu, 75 Paris 5<sup>e</sup>, France.

‡Swiss National Science Foundation Fellow.

<sup>1</sup>F. Herman, R. L. Kortum, I. Ortenburger, and J. P. Van Dyke, *J. Phys.* (Paris) Suppl. **29**, C4-62 (1968).

<sup>2</sup>L. E. Johnson, J. B. Conklin, Jr., and G. W. Pratt, Jr., *Phys. Rev. Lett.* **11**, 538 (1963); *Phys. Rev.* **137**, A1282 (1965).

<sup>3</sup>L. G. Ferreira, *Phys. Rev.* **137**, A1601 (1965).

<sup>4</sup>S. Rabii, *Phys. Rev.* **107**, 801 (1958); **173**, 918 (1968).

<sup>5</sup>H. Overhof and V. Rössler, *Phys. Status Solidi* **37**, 691 (1970).

<sup>6</sup>P. J. Lin and L. Kleinman, *Phys. Rev.* **142**, 478 (1966).

<sup>7</sup>R. L. Bernick and L. Kleinman, *Solid State Commun.* **8**, 569 (1970).

<sup>8</sup>Y. W. Tung and M. L. Cohen, *Phys. Rev.* **180**, 823 (1969); S. E. Kohn, P. Y. Yu, Y. Petroff, Y. R. Shen, Y. Tsang, and M. L. Cohen, *Phys. Rev. B* **8**, 1477

(1973).

<sup>9</sup>F. R. McFeely, S. Kowalczyk, L. Ley, R. A. Pollak, and D. A. Shirley, *Phys. Rev. B* **7**, 5228 (1973).

<sup>10</sup>M. Cardona, D. W. Langer, N. J. Shevchik, and J. Tejada, *Phys. Status Solidi B* **58**, 127 (1973).

<sup>11</sup>G. Martinez, M. Schlüter, and M. L. Cohen, following paper, *Phys. Rev. B* **11**, 660 (1975).

<sup>12</sup>M. L. Cohen and V. Heine, in *Solid State Physics*, edited by H. Ehrenreich, F. Seitz, and D. Turnbull (Academic, New York, 1970), Vol. 24, p. 37.

<sup>13</sup>F. Hermann, R. L. Kortum, C. D. Kuglin, J. P. Van Dyke, and S. Skillman, in *Methods in Computational Physics*, edited by B. Alder, S. Fernbach, and M. Rotenberg (Academic, New York, 1968), Vol. 8, p. 193, and references therein.

<sup>14</sup>D. Weaire, *Proc. Phys. Soc. Lond.* **92**, 956 (1967); M. Appapillai and V. Heine, Technical Report No. 5 (1972), Cavendish Laboratory, Cambridge (unpublished).

<sup>15</sup>F. Herman and S. Skillman, in *Atomic Structure Calculations* (Prentice-Hall, Englewood Cliffs, N. J., 1963).

<sup>16</sup>G. Weisz, *Phys. Rev.* **149**, 504 (1966).

<sup>17</sup>R. W. G. Wyckoff, *Crystal Structures* (Wiley, New

- York, 1963), Vol. 1.
- <sup>18</sup>S. I. Novikova and N. Kh. Abrikosov, *Fiz. Tverd. Tela* 5, 1913 (1963) [*Sov. Phys. -Solid State* 5, 1397 (1964)].
- <sup>19</sup>J. Chelikowsky and M. L. Cohen, *Phys. Rev. Lett.* 31, 1582 (1973); 32, 674 (1974); *Phys. Lett. A* 47, 7 (1974).
- <sup>20</sup>K. F. Cuff, M. R. Ellet, C. D. Kuglin, and L. R. Williams, *Proceedings of the Seventh International Conference on Physics of Semiconductors, Paris*, 1964, edited by M. Hulin (Dunod, Paris, 1964), p. 677.
- <sup>21</sup>G. Martinez, *Phys. Rev. B* 8, 4678 (1973).
- <sup>22</sup>J. Melngailis and T. C. Harman, *Phys. Rev. B* 5, 2250 (1972).
- <sup>23</sup>G. Martinez, M. Schlüter, and M. L. Cohen (unpublished).
- <sup>24</sup>D. L. Mitchell and R. F. Wallis, *Phys. Rev.* 151, 581 (1966).
- <sup>25</sup>J. Y. Leloup, B. Sapoval, and G. Martinez, *Phys. Rev. B* 7, 5276 (1973).
- <sup>26</sup>G. Martinez, M. Schlüter, and M. L. Cohen (unpublished).
- <sup>27</sup>G. Gillat and G. Dolling, *Phys. Lett.* 8, 304 (1964).